(impacting the potential for tDOC photooxidation), and water column stability and halocline development (*28*) will likely change the residence time and hence the fate of tDOC in the region. Further insights developed on the processes of tDOC removal in the Arctic will advance our understanding of tDOC sinks at lower latitudes, where the majority of the tDOC enters the global ocean.

### References and Notes

1. G. Cauwet, in *Biogeochemistry of Marine Dissolved Organic Matter*, D. A. Hansell, C. A. Carlson, Eds. (Academic Press, San Diego, CA, 2002), pp. 579–609.
2. R. F. C. Mantoura, E. M. S. Woodward, *Geochim. Cosmochim. Acta* **47**, 1293 (1983).
3. S. Opsahl, R. Benner, *Nature* **386**, 480 (1997).
4. J. I. Hedges, R. G. Keil, R. Benner, *Org. Geochem.* **27**, 195 (1997).
5. L. G. Anderson, in *Biogeochemistry of Marine Dissolved Organic Matter*, D. A. Hansell, C. A. Carlson, Eds. (Academic Press, San Diego, CA, 2002), pp. 665–683.
6. S. Opsahl, R. Benner, R. M. W. Amon, *Limnol. Oceanogr.* **44**, 2017 (1999).
7. P. A. Wheeler, J. M. Watkins, R. L. Hansing, *Deep-Sea Res. II* **44**, 1571 (1997).
8. R. M. W. Amon, in *The Arctic Ocean Organic Carbon Cycle*, R. Stein, R. W. Macdonald, Eds. (Springer, New York, 2003), pp. 83–99.
9. G. Kattner *et al.*, *Mar. Chem.* **65**, 25 (1999).
10. R. M. W. Amon, G. Budeus, B. J. Meon, *J. Geophys. Res.* **108**, 3221, 10.1029/2002JC001594 (2003).
11. J. Grebmeier, *Arct. Res. U.S.* **17**, 24 (2003).
12. R. W. Macdonald, F. A. McLaughlin, E. C. Carmack, *Deep-Sea Res. I* **49**, 1769 (2002).
13. K. Aagaard, E. C. Carmack, *J. Geophys. Res.* **94**, 14485 (1989).
14. C. K. H. Guay *et al.*, *J. Geophys. Res.* **106**, 11469 (2001).
15. M. J. Karcher, J. M. Oberhuber, *J. Geophys. Res.* **107**, 10.1029/2000JC000530 (2002).
16. D. Bauch, P. Schlosser, R. G. Fairbanks, *Prog. Oceanogr.* **35**, 53 (1995).
17. A. Fransson *et al.*, *Cont. Shelf Res.* **21**, 225 (2001).
18. C. K. H. Guay *et al.*, *Geophys. Res. Lett.* **26**, 1007 (1999).
19. J. M. Lobbes, H. P. Fitznar, G. Kattner, *Geochim. Cosmochim. Acta* **64**, 2973 (2000).
20. I. G. Droppo, D. Jeffries, C. Jaskot, S. Backus, *Arctic* **51**, 155 (1998).
21. M. M. Rutgers van der Loeff, R. M. Key, J. Scholten, D. Bauch, A. Michel, *Deep-Sea Res. II* **42**, 1533 (1995).
22. A. Kaufman, R. M. Trier, W. S. Broecker, H. W. Feely, *J. Geophys. Res.* **78**, 8827 (1973).
23. T. Dittmar, G. Kattner, *Mar. Chem.* **83**, 103 (2003).
24. R. Benner, B. Benitez-Nelson, R. M. W. Amon, *Geophys. Res. Lett.* **31**, L05305, 10.1029/2003GL019251 (2004).
25. B. J. Peterson, R. M. Holmes, J. W. McClelland, C. J. Voeroesmarty, *Science* **298**, 2171 (2002).
26. A. Y. Proshutinsky, M. A. Johnson, *J. Geophys. Res.* **102**, 12493 (1997).
27. C. Deser, J. E. Walsh, M. S. Timlin, *J. Clim.* **13**, 617 (2000).
28. M. Steele, T. Boyd, *J. Geophys. Res.* **103**, 10419 (1998).
29. The bathymetric map of the Arctic Ocean was prepared by M. Jakobsson, N. Z. Cherkis, J. Woodward, R. Mcnab, and B. Coakley, and is available at www.ngdc.noaa.gov/mgg/bathymetry/arctic/currentmap.html.
30. R. M. W. Amon, R. Benner, *Deep-Sea Res. I* **50**, 151 (2003).
31. Supported by the Arctic System Science Program, Office of Polar Programs, NSF (OPP-0124900, OPP-0124872, and OPP-0124868). We thank the crew and officers of the *USCGC Healy* as well as our SBI colleagues for their assistance in the collection of our data.

# Old World Fossil Record of Modern-Type Hummingbirds

**Gerald Mayr**

I report on tiny skeletons of stem-group hummingbirds from the early Oligocene of Germany that are of essentially modern appearance and exhibit morphological specializations toward nectarivory and hovering flight. These are the oldest fossils of modern-type hummingbirds, which had not previously been reported from the Old World. The findings demonstrate that early hummingbird evolution was not restricted to the New World. They further suggest that bird–flower coevolution dates back to the early Oligocene and open another view on the origin of ornithophily in Old World plants.

Today's hummingbirds (Apodiformes, Trochilidae) exclusively occur in the New World. Little is known about their early evolution (*1*), and the fossil record of the crown group, the clade that includes the stem species of the modern taxa and its descendants, is exceedingly poor, consisting of a small number of bones from the Quaternary of Central America (*2*, *3*). Although some apodiform birds from the early Tertiary of Europe and Asia were recently shown to be stem-group hummingbirds, i.e., hummingbirds outside the crown group (*4*), these are either very different from the modern taxa (*5*, *6*) or known from a few wing elements only (*7*). Here, I describe a taxon of stem-group hummingbirds from the early Oligocene of Germany that is of essentially modern appearance and exhibits morphological specializations toward nectarivory and hovering flight.

The classification of the species is Aves Linnaeus, 1758; Apodiformes Peters, 1940; Trochilidae Vigors, 1825; *Eurotrochilus inexpectatus* gen. et sp. nov. **Holotype.** SMNS (Staatliches Museum für Naturkunde, Stuttgart, Germany) 80739/4, partial disarticulated skeleton (Fig. 1). **Referred specimen.** SMNS 80739/3a+b, partial disarticulated skeleton on two slabs (Fig. 2). **Etymology**. *Euro*, for Europe, and *Trochilus*, the type genus of modern Trochilidae. The specific name is derived from Latin *inexpectatus* for unexpected and refers to the surprising occurrence of modern-type hummingbirds in Europe. **Type locality and horizon.** Frauenweiler south of Wiesloch (Baden-Württemberg, Germany), clay pit of the Bott-Eder GmbH ("Grube Unterfeld"); Rupelian, early Oligocene (30 to 34 million years ago) (*8–10*).

**Diagnosis.** *Eurotrochilus inexpectatus* is differentiated from all avian taxa except

Forschungsinstitut Senckenberg, Division of Ornithology, Senckenberganlage 25, D-60325 Frankfurt a.M., Germany. E-mail: Gerald.Mayr@senckenberg.de

**Table 1.** Length measurements and ratios of skeletal elements of fossil and extant hummingbirds. Measurements are given in millimeters; *P. pretrei*, *G. hirsuta*, and *C. mosquitus* are extant taxa.

| | Humerus | Ulna | Carpometacarpus | Tibiotarsus | Tarsometatarsus | Sternum | Sternum: ulna | Humerus: ulna |
|---|---|---|---|---|---|---|---|---|
| *E. inexpectatus*, holotype | 6.0 | 7.8* | — | 14.9 | 6.5 | 13.6 | 1.74 | 0.77 |
| *E. inexpectatus*, SMNS 80739/3 | — | 8.2 | 6.9 | — | 6.4 | 13.4* | 1.63 | — |
| *Jungornis tesselatus* | 8.0† | 13.0† | — | — | — | 13.8† | 1.06 | 0.62 |
| *Phaethornis pretrei* | 5.6 | 5.9 | 7.7 | 11.7 | 5.2 | 17.8 | 3.02 | 0.95 |
| *Glaucis hirsuta* | 6.0 | 7.3 | 8.4 | 13.2 | 5.2 | 20.2 | 2.77 | 0.82 |
| *Chrysolampis mosquitus* | 4.6 | 6.5 | 6.4 | 10.2 | 4.5 | 15.3 | 2.35 | 0.71 |

*Estimated　†Measurements after reference (*7*).

**Fig. 1.** *Eurotrochilus inexpectatus*, holotype SMNS 80739/4. (**A**) Specimen coated with ammonium chloride. (**B**) Enlarged view of coracoid and humerus. (**C**) Interpretative drawing. co, left coracoid; cra, cranium; fe, right femur; fm, foramen magnum; fu, furcula; hu, left humerus; man, mandible; max, maxillary bone; mpr, medial process at attachment site of musculus pronator superficialis; prt, distal protrusion on humeral head; qu, right quadrate; r, rib; sca, scapula; st, carina of sternum; sup, supracoracoideus nerve foramen; tbt, right tibiotarsus; tmt, right tarsometatarsus; ul, left ulna; v, vertebra.
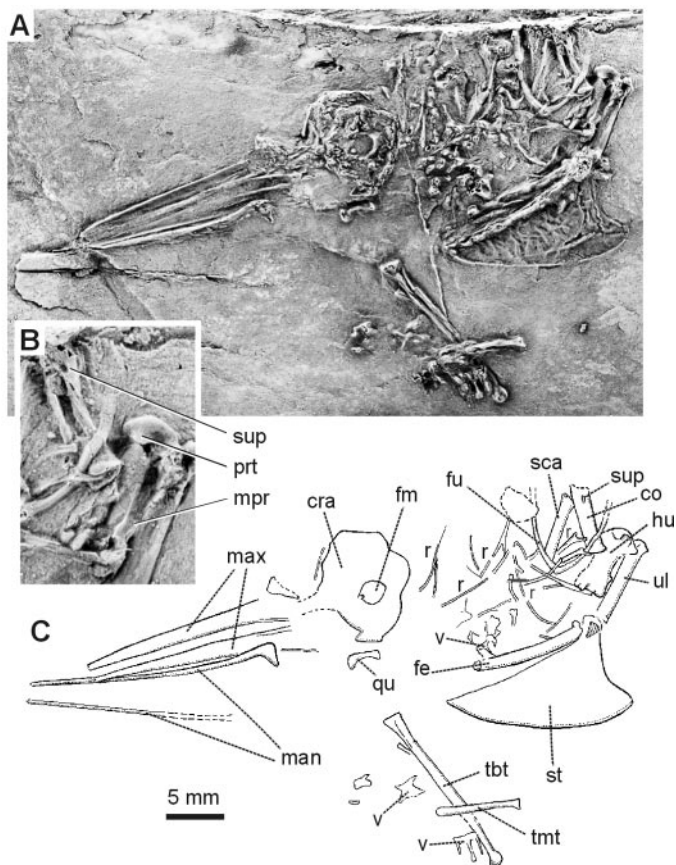
the early Oligocene stem-group hummingbird *Jungornis tesselatus* (*7*) and extant Trochilidae by the following derived characters: tiny size, humerus and ulna extremely abbreviated and stocky, pronounced distal protrusion on humeral head (Fig. 3), sternal end of coracoid columnlike with convex dorsal surface, and bill greatly elongated (unknown for *Jungornis*). *Eurotrochilus* is distinguished from *Jungornis* in its smaller size, a more strongly developed distal protrusion on the humeral head, and a proportionally more abbreviated ulna (Table 1). It is distinguished from crown-group Trochilidae in, for example, carpometacarpus without dentiform process, minor metacarpal distally not protruding beyond the major metacarpal, ulnar carpal with legs of markedly different length, and the shape of the internal index process on the proximal phalanx of the major digit (Fig. 3).

**Description.** *Eurotrochilus* is unequivocally identified as an apodiform bird by the derived proportions of its forelimb, in particular the greatly shortened and stout humerus and ulna (Fig. 3); there are no other avian taxa in which these bones are equally abbreviated. It is one of the smallest fossil birds, about the size of the extant rufous-breasted hermit *Glaucis hirsuta* (Trochilidae, Table 1), and thus distinctly smaller than any extant or fossil member of swifts, the sister taxon of hummingbirds (*11*, *12*). In concordance with
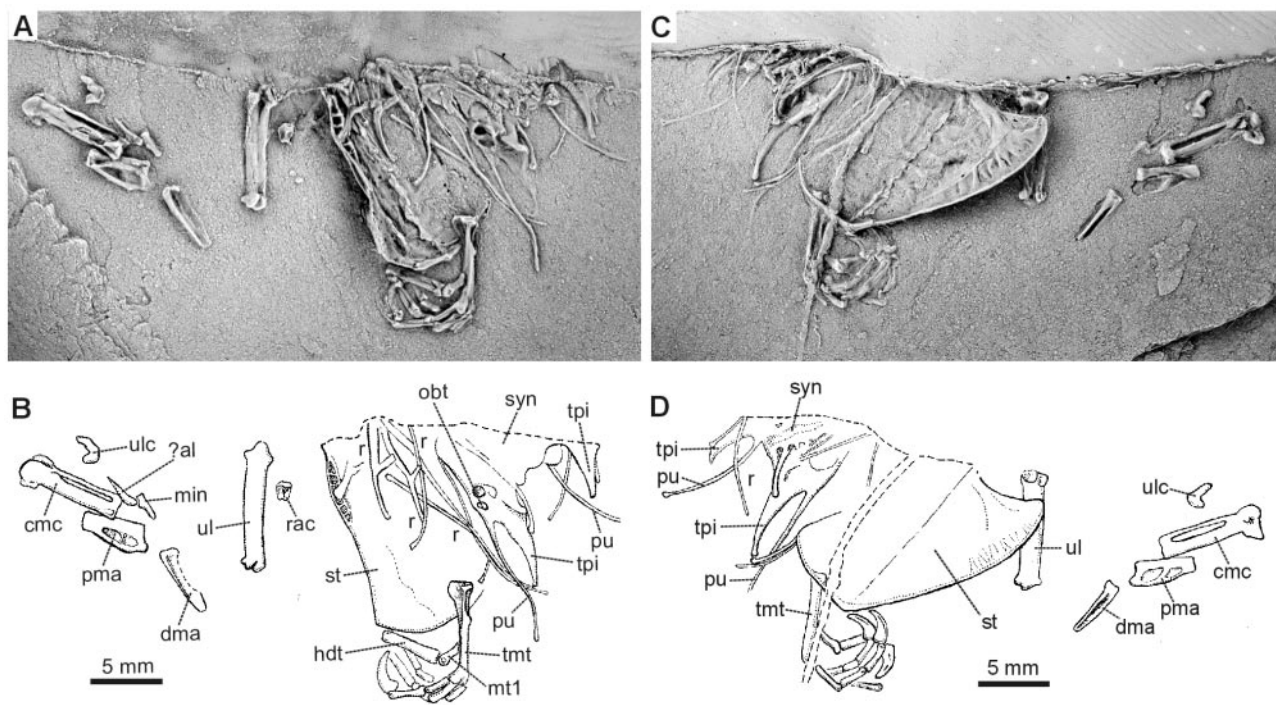


**Fig. 2.** *Eurotrochilus inexpectatus*, referred specimen. (**A**) SMNS 80739/3a, coated with ammonium chloride. (**B**) SMNS 80739/3a, interpretative drawing. (**C**) SMNS 80739/3b, coated with ammonium chloride. (**D**) SMNS 80739/3b, interpretative drawing. al, phalanx of alular digit; cmc, left carpometacarpus; dma, distal phalanx of major digit; hdt, hind toe; min, phalanx of minor digit; mt1, metatarsal of first toe; obt, obturator foramen; pma, proximal phalanx of major digit; pu, pubis; r, rib; rac, radial carpal; st, sternum; syn, synsacrum; tmt, left tarsometatarsus; tpi, terminal process of ischium; ul, ulna; ulc, ulnar carpal.

modern hummingbirds but contrary to swifts, which are aerial insectivores with a short and wide beak, *Eurotrochilus* has a derived, greatly elongated, and narrow beak that, although its distal part is not preserved in the holotype, still is about 2.5 times as long as the cranium (Fig. 1). As in extant Trochilidae, the maxillary processes of the palatine bone are widely separated, which indicates the presence of rhynchokinesis (*13*).

Another feature that shows *Eurotrochilus* to be a hummingbird is the highly derived morphology of the sternal extremity of the coracoid, which is columnlike with a convex dorsal surface and a greatly reduced lateral process (Fig. 1). In swifts, and virtually all other avian taxa, the coracoid becomes wider toward the more medially protruding sternal end. In concordance with other apodiform birds, the coracoid exhibits a large foramen for the supracoracoideus nerve (Fig. 1); the scapular end of this bone is not preserved in the specimen. The furcula is widely U-shaped, and the legs are very thin, as in modern hummingbirds. Also as in modern hummingbirds, the sternal carina is very high and the caudal margin of the corpus lacks any incisions. Although the sternum of *Eurotrochilus* is large, it is proportionally shorter than that of the extant taxa examined (Table 1). In agreement with the columnlike sternal extremity of the coracoid, the sternal articulation facet for the coracoid is not a narrow groove, as in nonapodiform birds, but a socket with a convex surface.

In its proportions, the humerus of *Eurotrochilus* resembles that of *Jungornis* from the early Oligocene of the Caucasus, which of the hitherto known stem-group taxa is the closest relative of modern hummingbirds (*4*). The humeral head bears a marked distal protrusion (Fig. 3) that is a distinctive apomorphy of a clade that includes *Jungornis* and modern Trochilidae (*4*) and that in modern hummingbirds is functionally related to the extreme supination of the adducted humerus during hovering flight (*6, 14*). In *Eurotrochilus*, this protrusion is more marked than in *Jungornis* and approaches the condition of extant Trochilidae. An additional apomorphy of a clade including *Jungornis* and modern Trochilidae that is also present in *Eurotrochilus* is the presence of a process on the medial side of the humerus (*4*) at the attachment site of the superficial pronator muscle (*6, 15*) (Fig. 3).

*Eurotrochilus* differs in a proportionally more abbreviated ulna from *Jungornis* (Table 1). Extreme abbreviation of the ulna unquestionably is derived within birds, and together with the more pronounced distal protrusion on the humeral head, supports monophyly of a clade that includes *Eurotrochilus* and crown-group Trochilidae, to the exclusion of *Jungornis*. There are no derived characters that are shared by *Eurotrochilus* and *Jungornis,* and not also present in modern Trochilidae, that would conflict with this classification. As in *Jungornis* and modern hummingbirds, the proximal end of the ulna bears a marked olecranal process (Fig. 3).

The hand, i.e., carpometacarpus and distal phalanges, distinctly exceeds the ulna in length (Fig. 3). The extensor process of the carpometacarpus protrudes more strongly than in extant hummingbirds, and the cranial margin of the bone further lacks a dentiform process (Fig. 3). Distally, the minor metacarpal does not extend beyond the major metacarpal. A small intermetacarpal process is present (Fig. 2), which is more strongly developed in modern hummingbirds but absent in swifts. The ulnar carpal is more asymmetric than the corresponding bone of modern hummingbirds (Fig. 3). The proximal phalanx of the major digit bears a large internal index process (*16*) that differs in its shape from the corresponding structure of extant hummingbirds, which is more pointed and triangular (Fig. 3). The phalanx of the minor digit is further not as greatly elongated as in modern hummingbirds (Fig. 3). These differences are due to the more derived morphology of crown-group Trochilidae and show *Eurotrochilus* to be a stem-group representative of Trochilidae.

Similar to other Apodiformes, the terminal processes of the ischium are very narrow, forming a large ischiopubic opening; the obturator foramen is caudally closed (Fig. 2). The tibiotarsus is poorly preserved in the holotype and is fairly long, with small cnemial crests. The short tarsometatarsus (Fig. 2) bears a large hypotarsus; the proximal part of its medial margin forms a sharp ridge. As in modern hummingbirds, the hind toe is long and attaches at the beginning of the distal third of the tarsometatarsus. The proximal phalanges of the anterior toes are not greatly abbreviated as in true swifts.

Although crown-group Trochilidae probably originated in South America (*17–19*), the fossil record now clearly shows that the evolution of the total group was not restricted to the New World. *Eurotrochilus* not only is the most convincing evidence for the presence of stem-group Trochilidae in the Old World Tertiary, but also indicates that there were even hummingbirds of essentially modern appearance in the early Oligocene of Europe.

The only other known beak of early Tertiary stem-group hummingbirds is swiftlike (*5*). *Eurotrochilus* exhibits a greatly elongated beak similar to that of modern hummingbirds, and the presence of a distal protrusion on the humeral head indicates that it was capable of hovering flight (*6, 14*). The combination of these two features strongly suggests that *Eurotrochilus* was nectarivorous, as are modern hummingbirds, in which case coevolution of birds and flowers (*20*) probably also goes back to the early Oligocene. *Eurotrochilus* provides the first evidence for nectarivory in early Tertiary stem-group hummingbirds and the earliest evidence for nectarivory in birds in general.

Most extant Old World nectarivorous birds belong to oscine songbirds (Passeriformes) (*21*), which are unknown in Europe before the end of the Oligocene (*22, 23*). (There is no early Tertiary fossil record of songbirds from Asia and Africa.) Hummingbird–flower coevolution might thus have predated songbird–flower coevolution in the Old World, and some ornithophilous Old World flowers that are now pollinated by the superficially hummingbird-like passeriform sunbirds (Nectariinidae) possibly stem from coevolution with hummingbirds in the early Tertiary.

Hummingbirds are the only group of birds in which most foraging is accomplished while hovering (*1*). Other nectarivorous birds normally make use of perches, and this difference in foraging modes is reflected in floral morphology of modern Neotropic and Palaeotropic ornithophilous plants (*24*). There are, however, a few flowers in the Old World that seem to be adapted to hovering avian pollinators but occur in areas without such birds, i.e., *Canarina eminii* (Campanulacea), *Impa-*
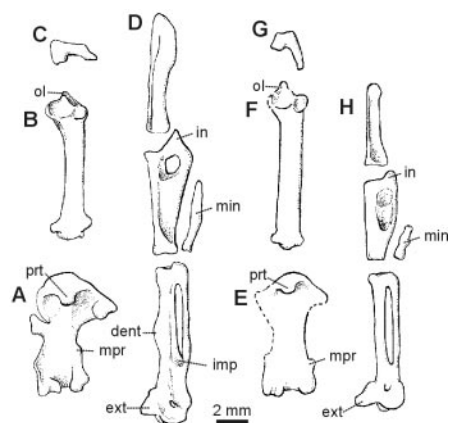


**Fig. 3.** Select wing elements of the extant rufous-breasted hermit *Glaucis hirsuta* (A to D) and *Eurotrochilus inexpectatus* (E to H). (**A** and **E**) Left humerus in caudal view (*Eurotrochilus* after SMNS 80739/4; dotted areas after *Jungornis*). (**B** and **F**) Left ulna in cranial view (*Eurotrochilus* after SMNS 80739/3). (**C** and **G**) Left ulnar carpal (*Eurotrochilus* after SMNS 80739/3). (**D** and **H**) Left hand in ventral view (*Eurotrochilus* after SMNS 80739/3). dent, dentiform process on carpometacarpus; ext, extensor process; imp, intermetacarpal process; in, internal index process on proximal phalanx of major digit; min, phalanx of minor digit; mpr, medial process at attachment site of musculus pronator superficialis; ol, olecranal process; prt, distal protrusion on humeral head.

*tiens sakeriana* (Balsaminaceae), and *Agapetes* spp. (Ericaceae) (*24*). It now has to be taken into consideration whether at least some of these go back to coevolution with early Tertiary stem-group hummingbirds. Many North American hummingbird flowers derive from bee-pollinated flowers (*25*), and after the disappearance of hummingbirds in the Old World, pollination of hummingbird flowers could have been taken over by insects, especially long-tongued bees (*26–28*).

### References and Notes

1. K. L. Schuchmann, in *Handbook of the Birds of the World, vol. 5*, J. del Hoyo, A. Elliot, J. Sargatal, Eds. (Lynx Edicions, Barcelona, 1999), pp. 468–680.
2. S. L. Olson, W. B. Hilgartner, *Smithson. Contrib. Paleobiol.* **48**, 22 (1982).
3. L. Bernstein, *Q. J. Fla. Acad. Sci.* **28**, 271 (1965).
4. G. Mayr, *Auk* **120**, 145 (2003).
5. G. Mayr, *Ibis* **145**, 382 (2003).
6. A. Karhu, *Smithson. Contrib. Paleobiol* **89**, 207 (1999).
7. A. Karhu, *Paleontol. Zh.* **3**, 78 (1988).
8. N. Micklich, N. Parin, *Publ. Espec. Inst. Esp. Oceanogr.* **21**, 129 (1996).
9. L. Trunkó, W. Munk, *Carolinea* **56**, 9 (1998).
10. S. Legendre, F. Lévêque, *Mém. Trav. EPHE Inst. Montpellier* **21**, 461 (1997).
11. C. G. Sibley, J. E. Ahlquist, *Phylogeny and Classification of Birds: A Study in Molecular Evolution* (Yale University Press, New Haven, CT, 1990).
12. U. S. Johansson, T. J. Parsons, M. Irestedt, P. G. P. Ericson, *J. Zool. Syst. Evol. Res.* **39**, 37 (2001).
13. R. L. Zusi, *Smithson. Contrib. Zool.* **395**, 1 (1984).
14. A. Karhu, in *Achievements and Problems of Ornithology of Northern Eurasia on a Boundary of Centuries*, E. Kurochkin, I. Rakhimov, Eds. (Margarif Publishers, Kazan, Tatarstan, 2001), pp. 118–132.
15. R. L. Zusi, G. D. Bentz, *Smithson. Contrib. Zool.* **385**, 1 (1984).
16. B. Stegmann, *J. Ornithol.* **104**, 413 (1963).
17. R. Bleiweiss, *Biol. J. Linn. Soc* **65**, 63 (1998).
18. R. Bleiweiss, *Biol. J. Linn. Soc.* **65**, 77 (1998).
19. A. Feduccia, *The Origin and Evolution of Birds* (Yale University Press, New Haven, CT, 1996).
20. E. J. Temeles, Y. B. Linhardt, M. Masonjones, H. D. Masonjones, *Biotropica* **34**, 68 (2002).
21. F. G. Stiles, *Ann. Miss. Bot. Gard.* **68**, 323 (1981).
22. C. Mourer-Chauviré, M. Hugueney, P. Jonet, *C. R. Acad. Sci. Paris* **309**, 843 (1989).
23. P. G. P. Ericson, M. Irestedt, U. Johansson, *J. Avian Biol.* **34**, 3 (2003).
24. C. Westerkamp, *Bot. Acta* **103**, 366 (1990).
25. V. Grant, *Proc. Natl. Acad. Sci. U.S.A.* **91**, 10407 (1994).
26. F. Stiles, *Am. Zool.* **18**, 715 (1978).
27. F. L. Carpenter, *Am. Zool.* **19**, 1105 (1979).
28. H. D. Bradshaw, D. W. Schemske, *Nature* **426**, 176 (2003).
29. I thank R. Böttcher (SMNS) for the loan of the fossil specimens, O. Vogel for the excellent preparation of the referred specimen, and S. Tränkner for taking the photographs. I further thank P. Houde and three anonymous referees for comments on the manuscript.

# Dioxygen Binds End-On to Mononuclear Copper in a Precatalytic Enzyme Complex

**Sean T. Prigge,[1,2] Betty A. Eipper,[3] Richard E. Mains,[3] L. Mario Amzel[2]***

Copper active sites play a major role in enzymatic activation of dioxygen. We trapped the copper-dioxygen complex in the enzyme peptidylglycine-alpha-hydroxylating monooxygenase (PHM) by freezing protein crystals that had been soaked with a slow substrate and ascorbate in the presence of oxygen. The x-ray crystal structure of this precatalytic complex, determined to 1.85-angstrom resolution, shows that oxygen binds to one of the coppers in the enzyme with an end-on geometry. Given this structure, it is likely that dioxygen is directly involved in the electron transfer and hydrogen abstraction steps of the PHM reaction. These insights may apply to other copper oxygen-activating enzymes, such as dopamine beta-monooxygenase, and to the design of biomimetic complexes.

Many peptide hormones and neuropeptides require amidation of their C terminus for biological activity (*1–3*). Peptidylglycine α-amidating monooxygenase (PAM) uses separate enzymatic domains to catalyze this amidation reaction in two steps: (i) hydroxylation of the Cα of a C-terminal glycine and (ii) disproportionation of the α-hydroxyglycine (*4, 5*). The first step is catalyzed by peptidylglycine α-hydroxylating monooxygenase (PHM), a two-copper, ascorbate-dependent enzyme that is the more extensively studied of the two PAM domains. Kinetic and mutagenesis studies (*6, 7*), detailed kinetic isotope effect measurements (*8–11*), and

extended x-ray absorption fine structure measurements (*7, 12–14*), as well as determination of the structures of several forms of the enzyme (*15, 16*), have been used in studying PHM. Despite these intense efforts, key aspects of the PHM mechanism remain elusive (*6, 17, 18*).

Perhaps the most puzzling aspect of the PHM reaction is the mechanism of electron transfer between the active-site coppers and the subsequent reduction of molecular oxygen. Each copper contributes one of the electrons required for the reduction of oxygen (*19*), but in all structures of PHM, the two active-site copper atoms ($Cu_A$ and $Cu_B$) are separated by a solvent-filled cleft about 11 Å wide—too far for direct electron transfer (*15, 16*). Crystallographic, spectroscopic, and kinetic studies have provided conflicting information about how electrons are transferred between the copper atoms, which copper atom is the binding site for molecular oxygen, and where the chemical steps of the PHM reaction take place. X-ray structures of

peptide substrate bound to PHM show that substrate binds with the glycine Cα in close proximity to $Cu_B$, indicating that $Cu_B$ is the likely site of oxygen binding and catalysis (*16*). Furthermore, bound substrate provides a path for the transfer of the electron from $Cu_A$ to $Cu_B$. Depending on the coordination of the dioxygen to $Cu_B$, the copper-bound oxygen may also be a part of the electron transfer path, coupling electron transfer to oxygen reduction and hydrogen abstraction.

Elucidation of the structure of PHM with bound peptide and oxygen could resolve some of these controversies, but this complex is difficult to study because it undergoes rapid catalysis, even in PHM crystals (*16*). Here we present the structure of the ternary complex of PHM with molecular oxygen and a peptide that contains a D-amino acid designed to trap the precatalytic complex. Formation of this complex required the preparation of reduced crystals ($Cu^I$) and stabilization of the substrate in the presence of reducing equivalents and oxygen. The structure obtained shows the positions of enzyme and substrate atoms immediately preceding catalysis and provides insight into the PHM mechanism.

We have previously shown that ascorbate will reduce $Cu_A$ and $Cu_B$ in crystalline PHM by demonstrating that PHM crystals can carry out multiple cycles of catalysis (*16*). However, the requirement for nickel in the crystallization solution raised the possibility that nickel could have replaced copper at either the $Cu_A$ or the $Cu_B$ site. We took advantage of the energy difference between the x-ray absorption edges of Cu (8979 eV) and Ni (8333 eV) to identify the metals in reduced and oxidized crystals of PHM.

Crystal diffraction data collected with x-ray energies of 8800 eV (1.409 Å) and 9000 eV (1.378 Å) can be used to distinguish between the metals at individual positions in the crystal. At 8800 eV, the imaginary com-

[1]Department of Microbiology and Molecular Immunology, The Bloomberg School of Public Health, [2]Department of Biophysics and Biophysical Chemistry, Johns Hopkins School of Medicine, Johns Hopkins University, Baltimore, MD, USA. [3]Department of Neuroscience, University of Connecticut Health Center, Farmington, CT, USA.

*To whom correspondence should be addressed. E-mail: Mario@neruda.med.jhmi.edu